

Computational Technologies for Brain Morphometry

Zicong Zhou*

Ben Hildebrandt[†]

Xi Chen[‡]

Guojun Liao[§]

October 10, 2018

Abstract

In this paper, we described a set of computational technologies for image analysis with applications in Brain Morphometry. The proposed technologies are based on a new Variational Principle which constructs a transformation with prescribed Jacobian determinant (which models local size changes) and prescribed curl-vector (which models local rotations). The goal of this research is to convince the image research community that Jacobian determinant as well as curl-vector should be used in all steps of image analysis. Specifically, we develop an optimal control method for non-rigid registration; a new concept and construction of average transformation; and a general robust method for construction of unbiased template from a set of images. Computational examples are presented to show the effects of curl-vector and the effectiveness of optimal control methods for non-rigid registration and our method for construction of unbiased template.

Keywords: Brain Morphometry, non-rigid registration, tensor based morphometry, Jacobian determinant, curl-vector, diffeomorphism

1 Introduction

In this paper, we address a key mathematical issue in brain morphometry which investigates variabilities in the shape and size of brain structures from image data. The issue is how to characterize diffeomorphisms. The prevailing paradigm in this field is to focus on Jacobian determinant $J(\mathbf{T})$ of the transformation \mathbf{T} , which models local size changes. We show that $J(\mathbf{T})$ alone cannot completely determine a transformation. Instead, we must use both $J(\mathbf{T})$ and the curl-vector of \mathbf{T} , $\text{curl}(\mathbf{T})$, which models local rotations, in all steps of brain morphometry studies. Specifically, we propose a new set of computational tools for morphometry studies.

- (1) For the non-rigid registration step, we develop an optimal control method which minimizes a dis-similarity measure (DS) under the constraints of partial differential equations such as $\text{div}(\mathbf{T}) = f$, $\text{curl}(\mathbf{T}) = g$ with respect to control functions f and g .
- (2) For the construction of an unbiased template, we propose an innovative concept of averaging a set of diffeomorphisms based on averaging the Jacobian determinants and curl-vectors of the diffeomorphisms.
- (3) For group differences, we propose to use Jacobian determinants and curl-vectors as features in TBM (tensor based morphometry) studies.

In this paper, we will focus on (1) and (2). We will demonstrate the effectiveness of our optimal control registration method mentioned in (1) and use it to perform the needed registration for constructing an unbiased template from a set of images in (2). In a future work, we will implement (3) in TBM (tensor based morphometry) studies of real data sets.

2 Effect of curl-Vectors, Variational Principle, Average of Transformations

The computational technologies described in this paper are based on a newly formulated Variational Principle [11]. We begin with an example to show the effects of the curl-vector.

*University of Texas at Arlington, Mathematics Department, Arlington, Texas 76019-0408, zicong.zhou@mavs.uta.edu

[†]University of Texas at Arlington, Mathematics Department, Arlington, Texas 76019-0408, ben.hildebrandt@mavs.uta.edu

[‡]University of Texas at Arlington, Mathematics Department, Arlington, Texas 76019-0408, xi.chen@mavs.uta.edu

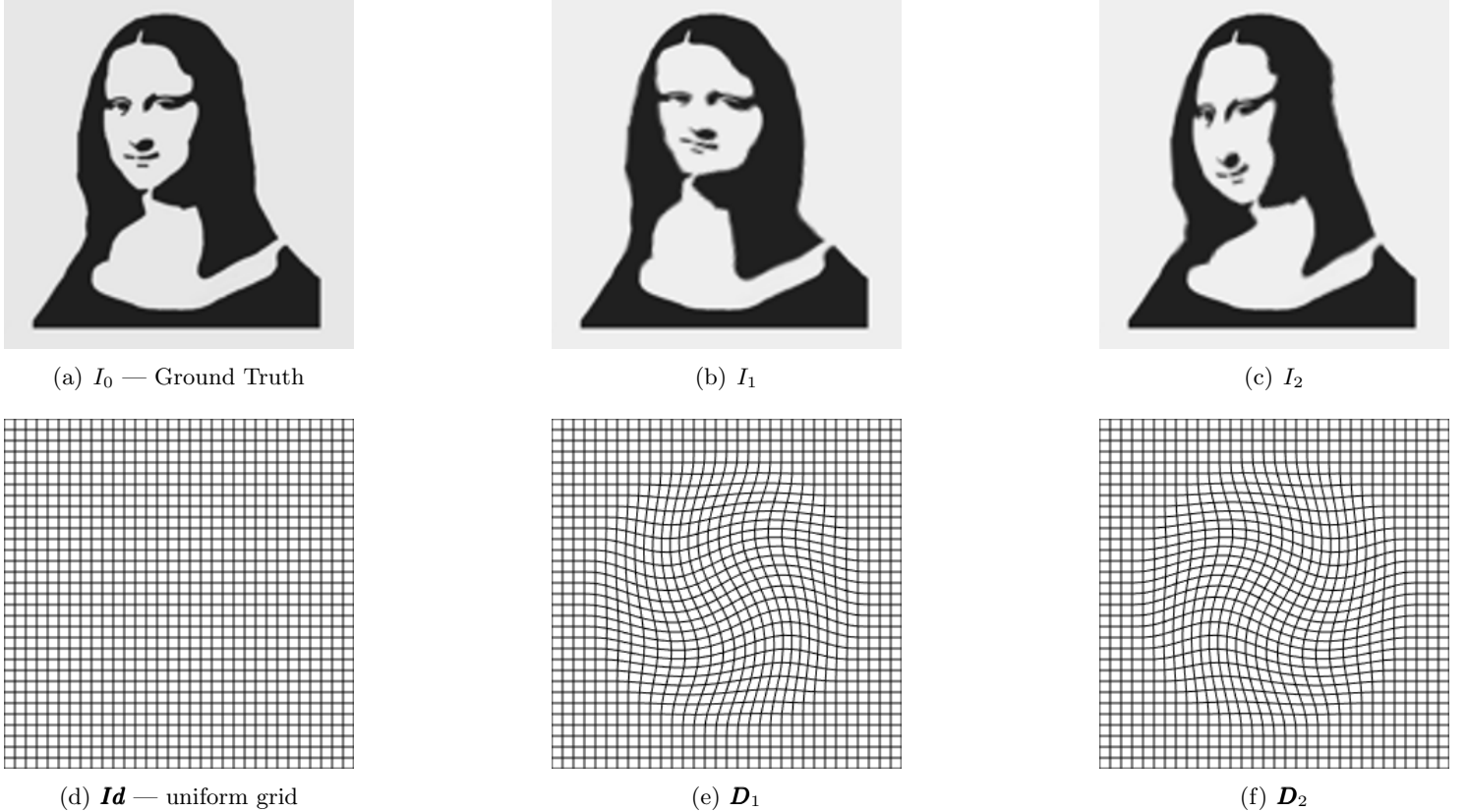
[§]University of Texas at Arlington, Mathematics Department, Arlington, Texas 76019-0408, liao@uta.edu

2.1 Effect of curl-Vectors

Started with a ground truth image (GT), based on portrait of Mona Lisa with 128*128 pixels shown in Figure 1(a). Then we generate two deformations \mathbf{D}_1 and \mathbf{D}_2 from the 128*128 uniform grid Figure 1(d) with spacing 1 (shown in 32*32) by opposite rotations such as that their Jacobian determinants are very close to 1 (in fact, between 0.996 and 1.003), and the average of their curl is 0 (the two rotations are cancelled). Figure 1(b) and 1(c) are the re-sampled images of Figure 1(a) on these two deformations Figure 1(e) and 1(f), respectively.

Resampling I_0 by \mathbf{D}_1 and \mathbf{D}_2 , which $J(\mathbf{D}_2) \cong 1 \cong J(\mathbf{D}_1)$ but $\text{curl}(\mathbf{D}_1) \neq \text{curl}(\mathbf{D}_2)$

Figure 1



2.2 Variational Principle

In this section, we describe the principles in 2D [11], where $\text{curl}(\mathbf{T})$ is a scalar function. A diffeomorphism \mathbf{T}_1 on a square domain \mathbb{D} can be deformed to \mathbf{T}_2 with prescribed Jacobian determinant $J(\mathbf{T}_2(\mathbf{x})) = f_0(\mathbf{x})$ and $\text{curl}(\mathbf{T}_2(\mathbf{x})) = g_0(\mathbf{x})$ in the interior of \mathbb{D} , and $\mathbf{T}(\mathbf{x}) = \mathbf{x}$ on the boundary of \mathbb{D} (f_0 is properly normalized for solvability). \mathbf{T}_2 is constructed by computational minimization of the functional:

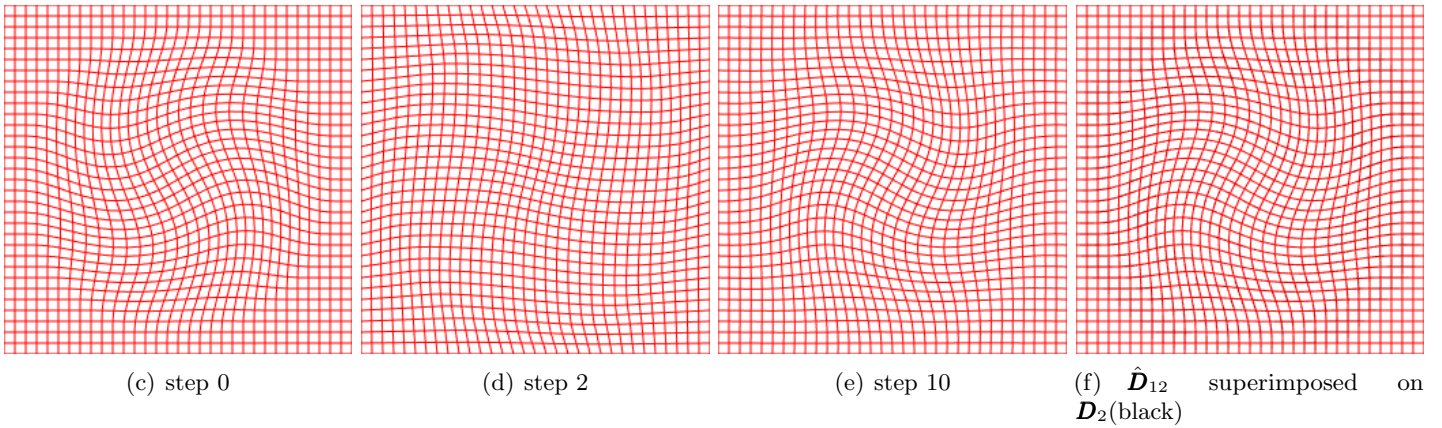
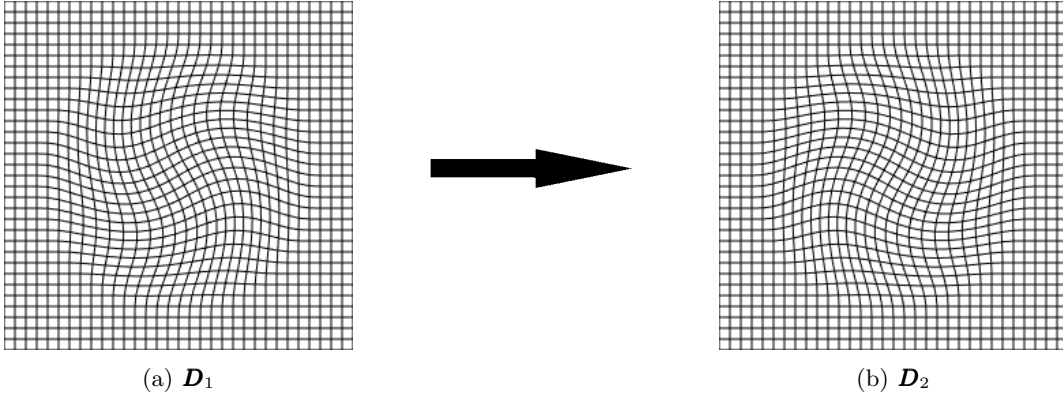
$$\iint_{\mathbb{D}} [(J(\mathbf{T}(\mathbf{x})) - f_0(\mathbf{x}))^2 + (\text{curl}(\mathbf{T}(\mathbf{x})) - g_0(\mathbf{x}))^2] d\mathbf{x} \quad (2.1)$$

subject to the constraints $\Delta \mathbf{T} = \mathbf{F}$. The variational problem is computed by a gradient decent method with respect to the control function $\mathbf{F} = (F_1, F_2)$. We demonstrate the principle in next two examples below.

Example 2: Numerical Performances of Variational Principal

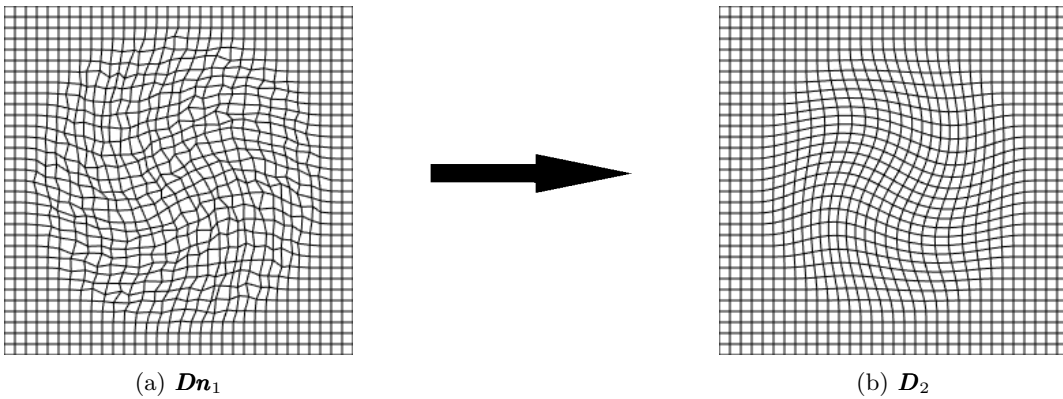
Deform \mathbf{D}_1 to \mathbf{D}_2 by the Variational Principle. Taking $f_0 = J(\mathbf{D}_2)$ and $g_0 = \text{curl}(\mathbf{D}_2)$ in the Variational Principle, in 25 iteration steps, \mathbf{D}_1 is deformed to a transformation — $\hat{\mathbf{D}}_{12}$, as shown in Figure 2(f) that is almost identical to \mathbf{D}_2 by prescribing its Jacobian as $J(\mathbf{D}_2)$ and its curl as $\text{curl}(\mathbf{D}_2)$. Total elapsed time for 25 iteration steps is 0.955899 seconds using a laptop.

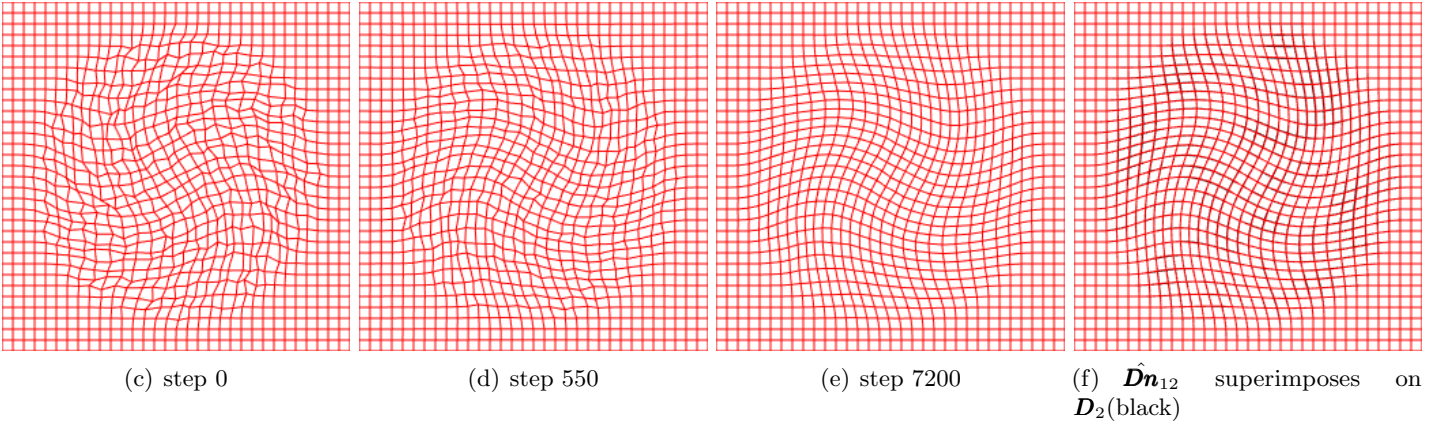
Figure 2: D_1 to D_2



We next add noise to D_1 and deform the distorted D_1 , denoted as Dn_1 , to D_2 as before. The calculated transformation \hat{Dn}_{12} (in red lines) by The Variational Principle is superimposed on D_2 as it shows in Figure 3(f). The red lines are almost identical to the black lines. This indicates that the results of the Variational Principle are very accurate.

Figure 3: Dn_1 to D_2





2.3 Average of Transformations

Based on the Variational Principle, we propose to average a set of transformations by averaging their Jacobian determinants and curl vectors. Given a set of transformations \mathbf{T}_i where $i = 1, 2, \dots, N$, we construct their average in the following steps:

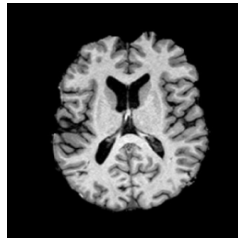
- (1) Let $f_0 = \frac{1}{N} \sum_i^N J(\mathbf{T}_i)$ and $g_0 = \frac{1}{N} \sum_{i=1}^N \text{curl}(\mathbf{T}_{i=1})$ as in [12]. (weighted averages can also be used)
- (2) Use f_0 and g_0 in the Variational Principle to calculate a transformation \mathbf{T} such that $J(\mathbf{T}) = f_0$ and $\text{curl}(\mathbf{T}) = g_0$.
- (3) We define this \mathbf{T} as the average of \mathbf{T}_i , where $i = 1, \dots, N$.

Our definition of average deformation has clear geometrical meaning: The local size change ratios modeled by $J(\mathbf{T}_i)$ and the local rotations modeled by $\text{curl}(\mathbf{T}_i)$ are averaged to determine the average deformation. These two geometrical features also are biologically meaningful: the Jacobian determinant models the tissue size changes; the curl vector models the local shape change. Moreover, we directly work with transformations and thus the method applies to different registration methods.

3 Construction of Unbiased Template

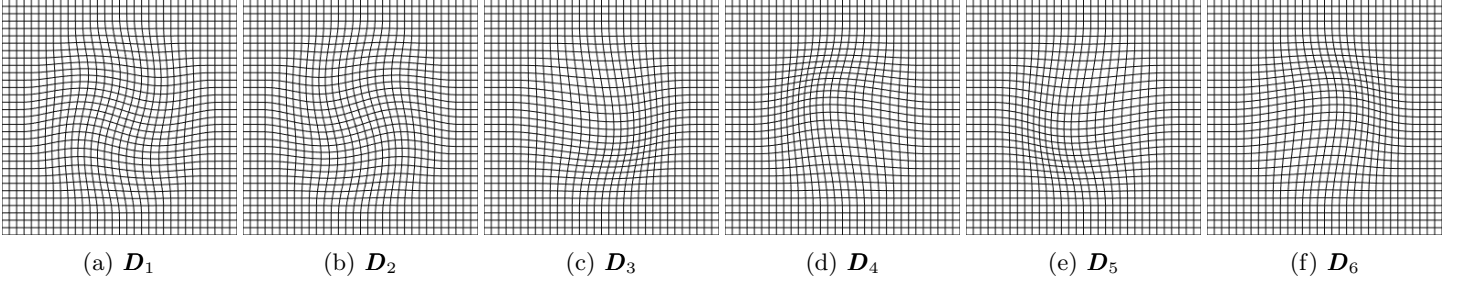
We propose a new method for construction of unbiased template from the members of an image set. The general method is described in Example 3 and a competitive computation friendly approach in Example 4. First, we obtain six brain images by re-sampling a ground truth brain image on six intentionally designed transformations \mathbf{D}_i , where $i = 1, \dots, 6$.

Figure 4: I_0 ground truth (GT) image



We constructed six transformations \mathbf{D}_i where $i = 1, \dots, 6$, which are shown below:

Figure 5: Transformations \mathbf{D}_{1-6}



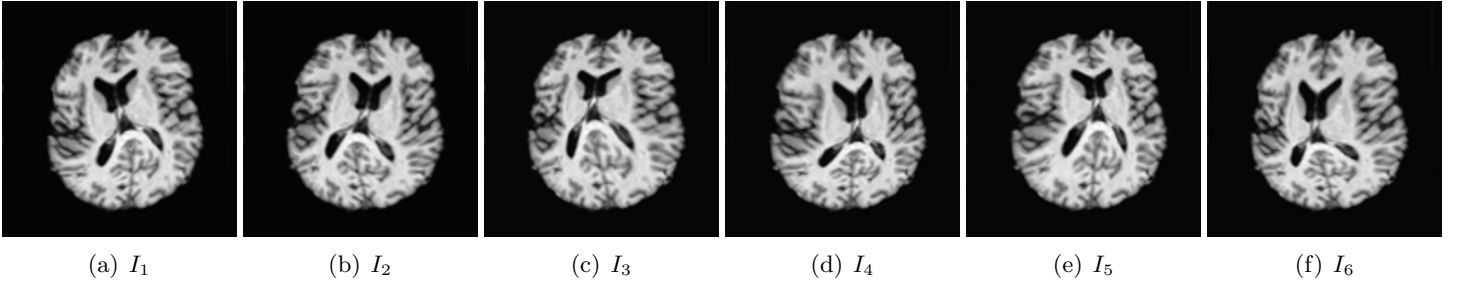
These transformations are constructed in such a way that their Jacobian determinants have average equal to 1, and their curls have average 0. In fact, we have

$$0.999986099590103 \leq \frac{1}{6} \sum_{i=1}^6 J(\mathbf{D}_i) \leq 1.000016719949570$$

$$-6.4029 * (10^{-6}) \leq \frac{1}{6} \sum_{i=1}^6 \text{curl}(\mathbf{D}_i) \leq 6.4029 * (10^{-6})$$

Six modeled brain images I_i , where $i = 1, \dots, 6$ are generated by re-sampling GT on each of the six transformations \mathbf{D}_i , where $i = 1, \dots, 6$. These images are shown Figure 6.

Figure 6: Image I_{1-6}

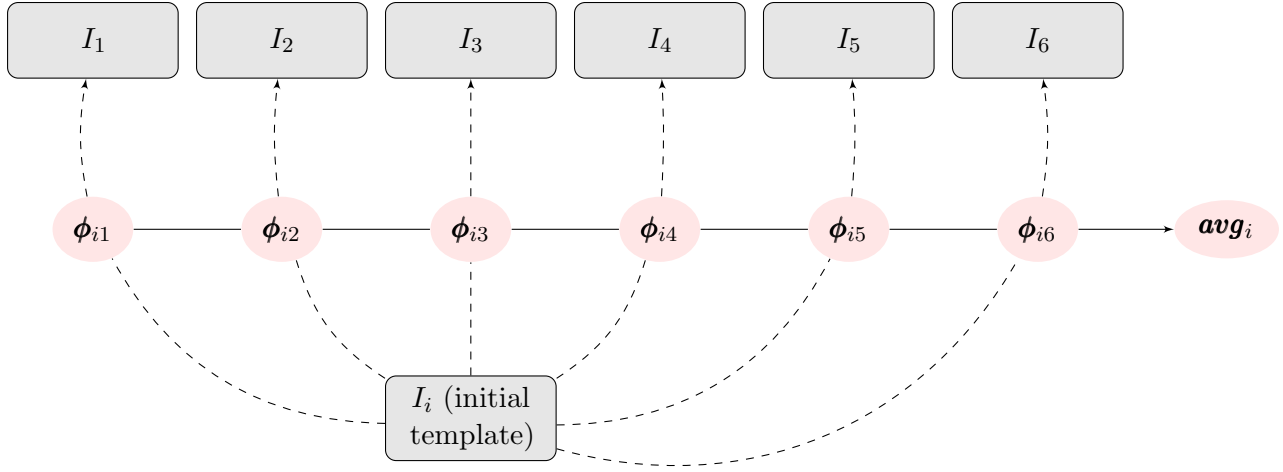


Now when we take $f_0 = \frac{1}{6} \sum_i^6 J(\mathbf{D}_i) \approx 1$ and $g_0 = \frac{1}{6} \sum_i^6 \text{curl}(\mathbf{D}_i) \approx 0$, by the Variational Principle, the average of these images is expected to be a good approximation to GT. We will verify this in Example 3. The Sum of Squared Differences (SSD) between I_i and GT — $SSD(I_i, I_0)$ (they can be seen as the initial difference from I_i to I_0) are shown in the following table:

i	1	2	3	4	5	6
$SSD(I_i, I_0) = (10^6)*$	1.8923	1.8906	1.8986	1.9610	1.8309	1.8353

Example 3: General Approach

In this example, we will walk through our method for the construction of unbiased template in a general sense. Step 1: take one image I_i out of the six images as the initial template, then register I_i to all six images I_j for $j = 1, 2, \dots, 6$ (arrowed dash-lines) to find six registration transformations — ϕ_{ij} for $j = 1, 2, \dots, 6$; Step 2: find the average transformation $\mathbf{avg}_i = \text{avg}(\phi_{ij=1, \dots, 6})$ of the six registration deformations by the Variational Principle (arrowed solid-line), as are demonstrated in the following diagram.



Step 3, re-sample I_i on the average transformation \mathbf{avg}_i , indicated as the next diagram and shown in Figure 7, to get the biased temporary templates $\hat{Template}_i = I_i(\mathbf{avg}_i)$ for each $i = 1, 2, \dots, 6$ which are shown in Figure 8.



Figure 7: Average transformation — $\mathbf{avg}_i = \text{avg}(\phi_{ij=1,\dots,6})$

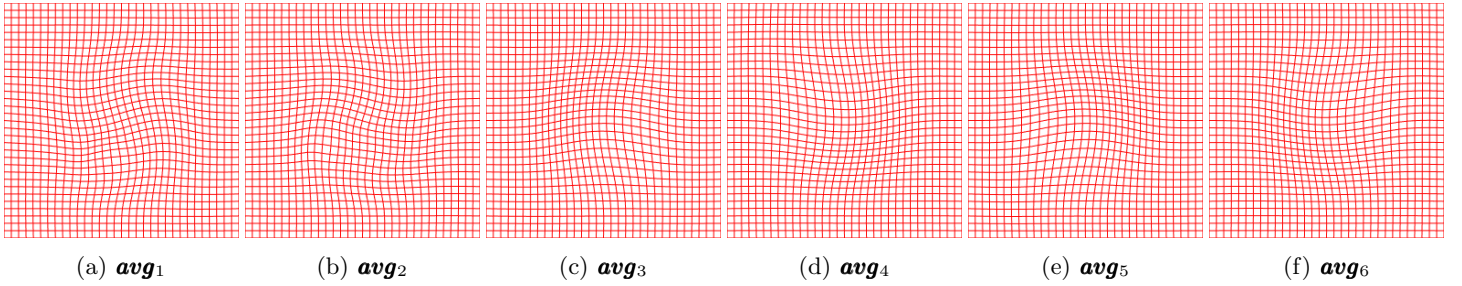
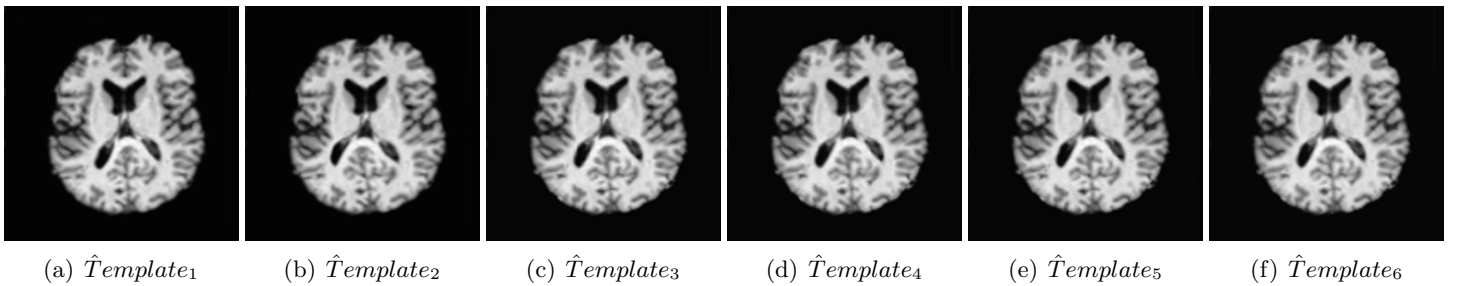


Figure 8: Biased Temporary Templates — $\hat{Template}_i = I_i(\mathbf{avg}_i)$



The SSD between \hat{I}_i with the GT — $SSD(\hat{Template}_i, I_0)$ and $Error_i = \frac{SSD(\hat{Template}_i, I_0)}{SSD(I_i, I_0)}$ are shown in the following table. $Error_i$ measures the error reduction in temporary template $\hat{Template}_i$ compared to the image I_i .

i	1	2	3	4	5	6
$SSD(\hat{Template}_i, I_0) = (10^6)*$	2.0504	3.4073	0.4963	0.4905	0.4835	0.5116
$Error_i$	0.1084	0.1802	0.0261	0.0250	0.0264	0.0279

As it can be seen, $\hat{Template}_2$ has the highest error = 0.1802. At this stage, $\hat{Template}_4$ is the best with an error 0.0250 (this means 97.5% of the initial SSD between image I_4 and GT is reduced by our optimal control

registration method). The large difference between $Error_2 = 0.1802$ and $Error_4 = 0.0250$ indicates the existence of bias towards the image that is used as an initial template. In order to quantify the bias, we calculate the sample mean and standard deviation of the six $SSD(\hat{Template}_i, I_0)$'s: Sample Mean = $1.2400 * (10^6)$, Sample Standard Deviation = $1.2306 * (10^6)$. So, $SSD(\hat{Template}_6, I_0)$ is the closest to the Sample Mean. But the large standard deviation of this sample disqualifies any one of these templates as unbiased.

This leads to Step-4: repeat Step-1 to Step-3 on biased temporary templates — $\hat{Template}_i$ to reduce their bias. So we get a new group of average transformation Avg_i as shown in Figure 9 and the re-sampled images are the Unbiased Templates — $Template_i = \hat{Template}_i(Avg_i)$ as shown in Figure 10.

Figure 9: Average transformation — Avg_i

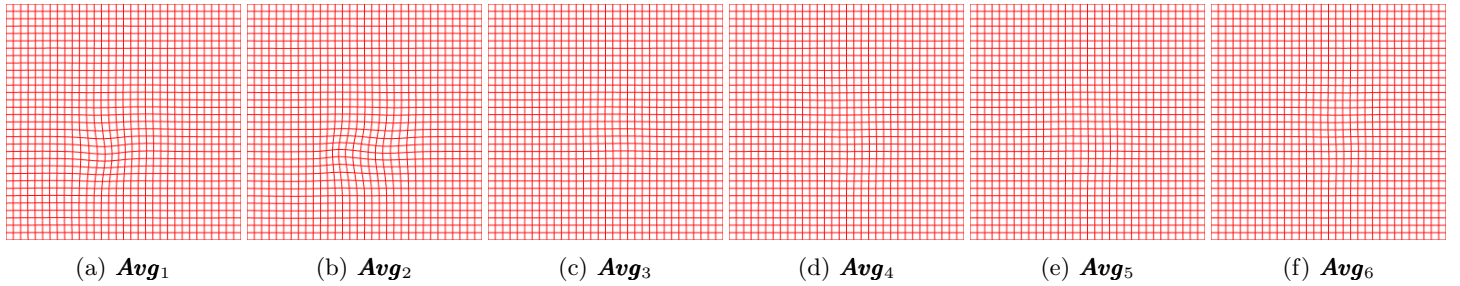
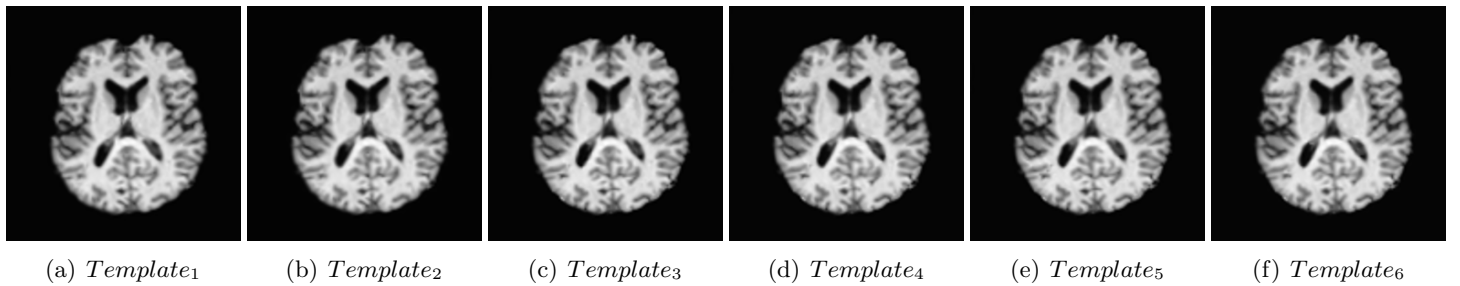


Figure 10: Unbiased Templates — $Template_i = \hat{Template}_i(Avg_i)$

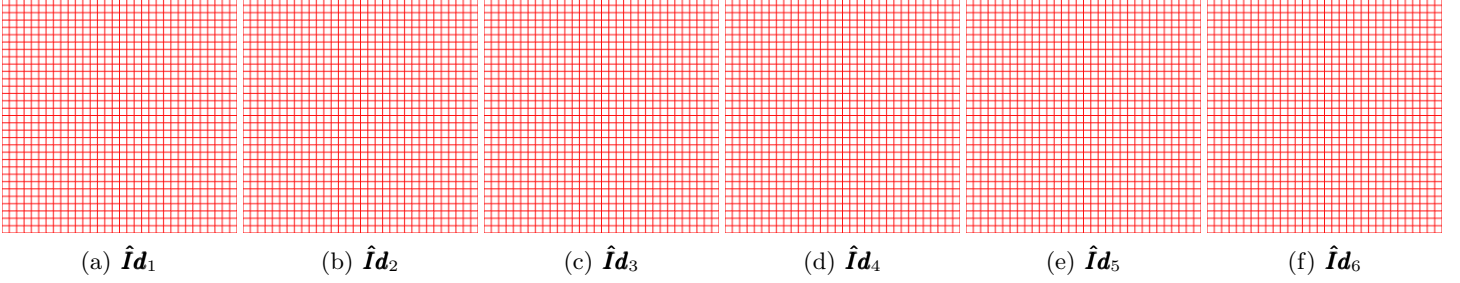


The SSD between $Template_i$ with the GT — $SSD(Template_i, I_0)$ and $Error_i = \frac{SSD(Template_i, I_0)}{SSD(I_i, I_0)}$ are shown in the following table which measures the error reduction in temporary template $Template_i$ compared to the image I_i .

i	1	2	3	4	5	6
$SSD(Template_i, I_0) = (10^5)*$	6.7786	6.6041	5.5583	5.6649	5.7469	5.8088
$Error_i$	0.0358	0.0349	0.0292	0.0289	0.0314	0.0317

The statistics are significantly improved: New Sample Mean = $6.0269 * (10^5)$; New Sample Standard Deviation = $5.2436 * (10^4)$. $Template_6$ is closest to the New Sample Mean. The New Sample Standard Deviation = $5.2436 * (10^4)$ is now only 4.3566% of the previous Sample Standard Deviation = $1.2306 * (10^6)$. This means, the effectiveness of repeating Step-1 to Step-3 on the biased temporary templates has greatly reduced the bias of biased temporary template $\{\hat{Template}_i\}$. Hence, we can take any of the new templates $Template_i$ as an unbiased template. To check that, we may register each of $Template_i$ to I_0 to get six register transformations and all of them are expected to be close to the identity map Id as the results are shown in Figure 11.

Figure 11: Average transformation — $\hat{\mathbf{I}}\mathbf{d}_i$



And the behaviors of their Jacobian determinant and curl are shown in the following table.

i	1	2	3	4	5	6
$\max J(\hat{\mathbf{I}}\mathbf{d}_i)$	1.0000	1.0000	1.0000	1.0000	1.0000	1.0000
$\min J(\hat{\mathbf{I}}\mathbf{d}_i)$	0.9999	0.9999	0.9999	0.9999	0.9999	0.9999
$\max \text{curl}(\hat{\mathbf{I}}\mathbf{d}_i) = 10^{-14}_*$	0.3553	0.3553	0.1776	0.1776	0.3553	0.3553
$\min \text{curl}(\hat{\mathbf{I}}\mathbf{d}_i) = 10^{-14}_*$	-0.3553	-0.3553	-0.1776	-0.1776	-0.3553	-0.3553

Example 4: Computation Friendly Approach

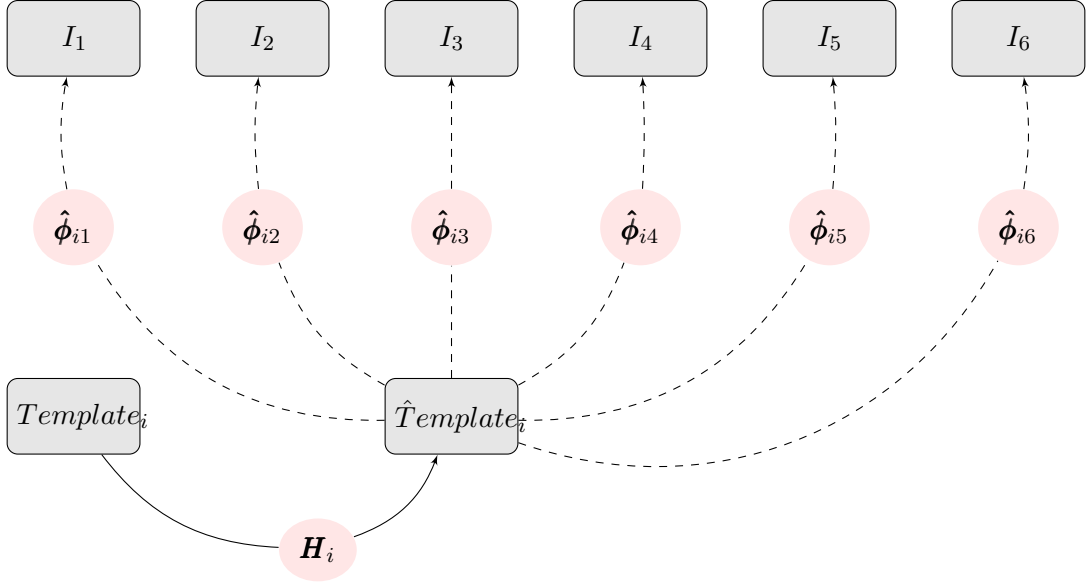
In Example 3, the crucial part is Step-3 for our general approach of constructing an unbiased template, which requires to find all $\hat{T}emplate_i$ for all $i = 1, \dots, 6$ and it is not a cheap task to do in terms of computational costs. In this example, we construct a correction transformation to reduce the bias of any initial template I_i , by using an approximation to composition of small deformations, which “allows” us to do a similar job without finding all $\hat{T}emplate_i$. This can be done under the assumption that ground-truth Jacobian determinant and curl-vector are known.

Let’s take one of the I_i as the initial template, then we perform Step-1 and Step-2 as they were in Example 3, to get an biased temporary template $\hat{T}emplate_i$. To see the process is independent of choosing initial template, we will show the results of all six image I_i as the initial template individually.

Correction transformation \mathbf{H}_i ’s

We have derived a mathematical formula to generate correction transformations \mathbf{H}_i ’s for each of $\hat{T}emplate_i$ where $i = 1, \dots, 6$. Let $\{I_i\}$ be the given images and $\{\hat{T}emplate_i\}$ be the temporary templates by above procedures. As it can be seen in Example 3, using I_1 and I_2 to form the temporary templates would give strongly biased results. Therefore, in order to construct unbiased template, a correction transformation \mathbf{H}_i needs to be introduced which depends on the initial template I_i .

To construct \mathbf{H}_i (arrowed solid-line on the diagram) for a fixed i : Firstly, applying our image registration method to find registration transformations $\hat{\phi}_{i,j} : \hat{T}emplate_i \rightarrow I_j, \forall j = 1, 2, \dots, N$ (arrowed dash-line on the diagram). Let consider the following diagram:



The construction of biased temporary templates $\hat{T}emplate_i$ are actually expected to be the unbiased template $Template_i$ in Step-1 and Step-2 of Example 3. Due to computational limitations, they did not reduce the bias enough, so we got only a biased temporary template $\hat{T}emplate_i$. However, the original bias of the initial template I_i has been reduced to a level that makes the temporary templates $\hat{T}emplate_i$ closer to I_0 than the initial template I_i . We would like to ask, does it exist a small deformation $\mathbf{H}_i(\mathbf{x})$ that deforms the unbiased template $Template_i$ to $\hat{T}emplate_i$? If it exists, how to find it?

Secondly, according to our definition of unbiased template, if \mathbf{H}_i exists, then it must satisfy the following equations:

$$\begin{cases} \frac{\sum_{j=1}^N J(\hat{\phi}_{ij} \circ \mathbf{H}_i(\mathbf{x}))}{N} = 1 \\ \sum_{j=1}^N \text{curl}(\hat{\phi}_{ij} \circ \mathbf{H}_i(\mathbf{x})) = 0 \end{cases} \quad (3.1)$$

This means, if there exists an unbiased template which should be almost identical to GT — I_0 , then the each compositions of $\hat{\phi}_{ij} \circ \mathbf{H}_i$ should behaves very close to the inverse transformation of \mathbf{D}_i , where \mathbf{D}_i were shown in Figure 5. Therefore the average of $J(\hat{\phi}_{ij} \circ \mathbf{H}_i(\mathbf{x}))$ should be 1 and the average $\text{curl}(\hat{\phi}_{ij} \circ \mathbf{H}_i(\mathbf{x}))$ should be 0 for each i .

By property $J(\mathbf{T}_2 \circ \mathbf{T}_1) = J(\mathbf{T}_1)J(\mathbf{T}_2)$, we know

$$\frac{\sum_{j=1}^N J(\hat{\phi}_{ij} \circ \mathbf{H}_i(\mathbf{x}))}{N} = J(\mathbf{H}_i(\mathbf{x})) \frac{\sum_{j=1}^N J(\hat{\phi}_{ij}(\mathbf{x}))}{N} = 1 \quad \implies \quad J(\mathbf{H}_i(\mathbf{x})) = \frac{N}{\sum_{j=1}^N J(\hat{\phi}_{ij}(\mathbf{x}))} \quad (3.2)$$

$\mathbf{H}_i(\mathbf{x})$ is small deformation and it can be represented as $\mathbf{H}_i(\mathbf{x}) = \mathbf{x} + \mathbf{u}_i(\mathbf{x})$, therefore, we have

$$\text{curl}(\mathbf{H}_i(\mathbf{x})) = \text{curl}(\mathbf{u}_i(\mathbf{x})) \quad (3.3)$$

And composition of two small deformations, let $\mathbf{T}_1(\mathbf{x}) = \mathbf{x} + \mathbf{u}_1(\mathbf{x})$ and $\mathbf{T}_2(\mathbf{x}) = \mathbf{x} + \mathbf{u}_2(\mathbf{x})$ where $\mathbf{u}_i(\mathbf{x})$ are displacement fields, can be approximated [5] by

$$\mathbf{T}_2 \circ \mathbf{T}_1(\mathbf{x}) \approx \mathbf{x} + \mathbf{u}_1(\mathbf{x}) + \mathbf{u}_2(\mathbf{x}) = \mathbf{x} + \mathbf{u}_2(\mathbf{x}) + \mathbf{u}_1(\mathbf{x}) = \mathbf{T}_2(\mathbf{x}) + \mathbf{u}_1(\mathbf{x})$$

this leads to

$$\mathbf{H}_i \circ \hat{\phi}_{ij}(\mathbf{x}) \approx \hat{\phi}_{ij}(\mathbf{x}) + \mathbf{u}_i(\mathbf{x})$$

Therefore, by (3.3), we have

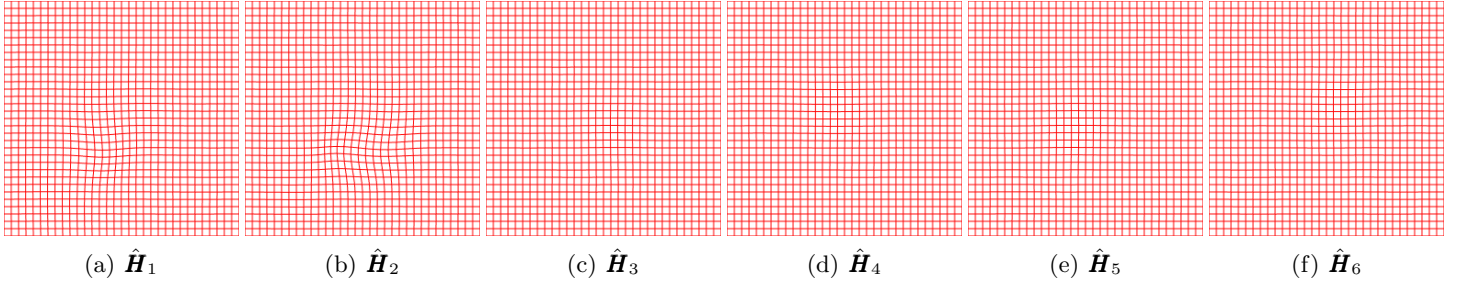
$$\text{curl}(\mathbf{H}_i \circ \hat{\phi}_{ij}(\mathbf{x})) \approx \text{curl}(\hat{\phi}_{ij}) + \text{curl}(\mathbf{u}_i(\mathbf{x})) = \text{curl}(\hat{\phi}_{ij}) + \text{curl}(\mathbf{H}_i(\mathbf{x})) \quad (3.4)$$

Now, by (3.2) and (3.4), the approximations of Jacobian determinant and curl of \mathbf{H}_i in (3.1), denoted as $J(\hat{\mathbf{H}}_i(\mathbf{x}))$ and $\text{curl}(\hat{\mathbf{H}}_i(\mathbf{x}))$, respectively, which are in the form of

$$\begin{cases} J(\hat{\mathbf{H}}_i(\mathbf{x})) = \frac{N}{\sum_{j=1}^N J(\hat{\phi}_{ij}(\mathbf{x}))} \\ \text{curl}(\hat{\mathbf{H}}_i(\mathbf{x})) = \frac{-\sum_{j=1}^N \text{curl}(\hat{\phi}_{ij}(\mathbf{x}))}{N} \end{cases} \quad (3.5)$$

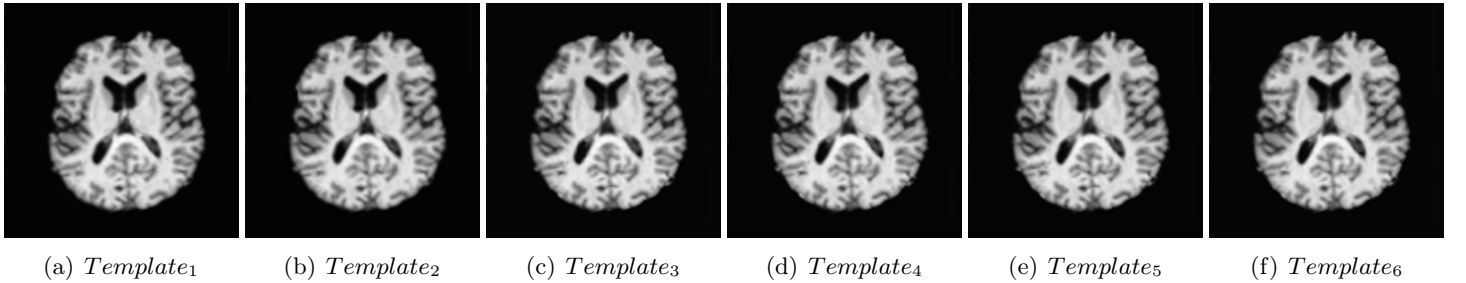
Finally, we find $\hat{\mathbf{H}}_i$ by our Variational Principle. The approximated transformations $\hat{\mathbf{H}}_i$'s are shown in Figure 12.

Figure 12: Correction Transformation, $\hat{\mathbf{H}}_{1-6}$



After re-sampling each $\hat{T}emplate_i$ on transformation $\hat{\mathbf{H}}_i$'s, we obtain a set of six new templates $Template_i$ as shown in Figure 13, which are much more uniform now.

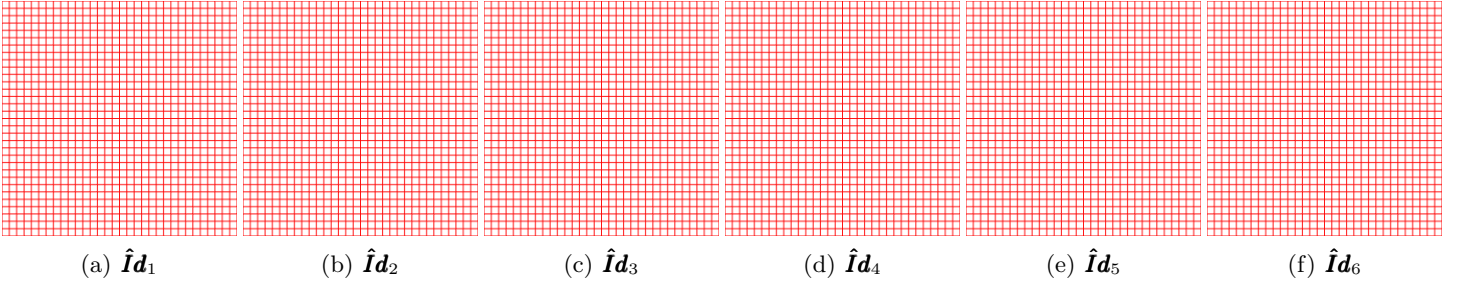
Figure 13: Unbiased Templates — $Template_i$



Similarly as the results from Example 3, the highest error is 0.0372, downed from 0.1802. The SSD between new templates $Template_i$'s and I_0 are reduced by an order of 10 as $SSD(Template_i, I_0)$ and $Error_i = \frac{SSD(Template_i, I_0)}{SSD(I_i, I_0)}$ shown in the table. It measures the relative error in the new template $Template_i$ compared to the image I_i .

i	1	2	3	4	5	6
$SSD(Template_i, I_0) = (10^5)*$	6.6972	7.0447	5.0143	4.9911	5.0290	5.2408
$Error_i$	0.0354	0.0372	0.0264	0.0254	0.0274	0.0286

The statistics are also significantly improved just like in the results in Example 3: New Sample Mean = $5.6695 * (10^5)$; New Sample Standard Deviation = $9.4137 * (10^4)$. $Template_6$ is closest to the New Sample Mean. The New Sample Standard Deviation = $9.4137 * (10^4)$ is now only 7.65% of the previous Sample Standard Deviation = $1.2306 * (10^6)$. This means, with the help of approximated correction transformations $\hat{\mathbf{H}}_i$, we have greatly reduced the bias. And $\hat{\mathbf{H}}_i$ has been a good approximation to \mathbf{H}_i . To check that, we registered $Template_i$ to I_0 for each i , denoted as $\hat{\mathbf{I}}d_i$ which are shown in next Figure 14. They are expected to be close to the identity map \mathbf{Id} . Therefore, we can take any of the new templates $Template_i$ as an unbiased template.

Figure 14: $\hat{\mathbf{I}}\mathbf{d}_i$ 

i	1	2	3	4	5	6
$\max J(\hat{\mathbf{I}}\mathbf{d}_i)$	1.0000	1.0000	1.0000	1.0000	1.0000	1.0000
$\min J(\hat{\mathbf{I}}\mathbf{d}_i)$	0.9999	0.9999	0.9999	0.9999	0.9999	0.9999
$\max \text{curl}(\hat{\mathbf{I}}\mathbf{d}_i) = 10^{-14}_*$	0.3553	0.3553	0.1776	0.1776	0.1776	0.1776
$\min \text{curl}(\hat{\mathbf{I}}\mathbf{d}_i) = 10^{-14}_*$	-0.3553	-0.3553	-0.1776	-0.1776	-0.1776	-0.1776

4 Optimal Control Method for Non-rigid Image Registration

In this section, we describe the image registration method that we used to calculate the examples. Image registration is the process of establishing pixel (voxel) correspondence between two or more images so that certain similarity measure is maximized, or a dis-similarity measure (DS) is minimized. The images can be taken from the same individual at different posts and different times; or from different individuals. The images can also be in different modalities.

Over last decades, many sophisticated methods have been developed. Most of these methods regularize the ill-posed registration problem by various penalty terms that are either based on physical models or geometric considerations. The cost to be minimized is the sum of DS and the regularizing term Reg : $C = DS + \alpha Reg$, where α is a parameter controlling the trade-off between the data term DS and the regularizing term Reg . There are two issues with this framework:

- (1) the addition of the second term distorted the problem; For instance, the regularizing term changed the optimal transportation flow to be non-gradient flow.
- (2) The determination of the value of α is more like an art than science. If it is too large, the registration transformation becomes too smooth; while if it is too small the computation becomes unstable.

Some methods introduce regularization implicitly. For instance, the splines-based method minimizes DS on a coarse grid (say 8 by 8 pixels are represented in a grid cell) whose nodes are the control points for splines. After the new locations of the control points are determined, locations of the remaining pixels are interpolated by the splines formulas.

In [4, 6] we proposed an optimal control approach that has no explicit penalty terms (and hence no parameters). Instead, we minimize DS subject to the constraints $\mathcal{L}[\mathbf{u}] = \mathbf{F}$ with respect to the control function \mathbf{F} . The registration transformation \mathbf{T} is iteratively determined: at the $k + 1$ step, $\mathbf{T}^{k+1}(\mathbf{x}) = \mathbf{T}^k(\mathbf{x} + \mathbf{u}^{k+1})$. \mathcal{L} is a partial differential operator providing regularity. For instance, in 2D, we can take $\text{div}(\mathbf{u}) = F_1$, and $\text{curl}(\mathbf{u}) = F_2$. Or we can simply take $\Delta \mathbf{u} = \mathbf{F}$. In the version described in [4], there is a mechanism that keeps the Jacobian determinant positive, which in turn assures that \mathbf{T} is a diffeomorphism (invertible and smooth).

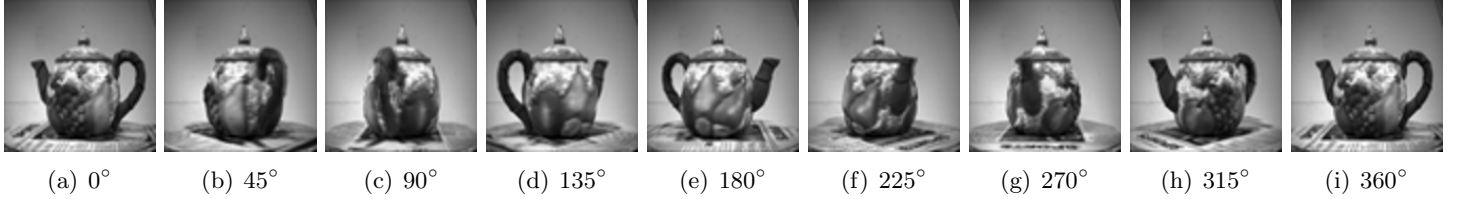
The optimal control approach is inspired by the success of fluid control algorithms. The variational problem is solved by the gradient decent method. As indicated in the survey paper [9], one could add a penalty term to DS for specific application with a small parameter value α in order to use prior knowledge. We now present a teapot example.

Example 5: Registration of 3D Teapot Images by Optimal Control Method

We now describe the volume image I_0 and the twisted image I_t in Step-1. In Step-2, we register I_t to I_0 , and output the registration transformation and the deformed image I_t . The results show that the twisted image I_t is deformed back to the I_0 with high accuracy.

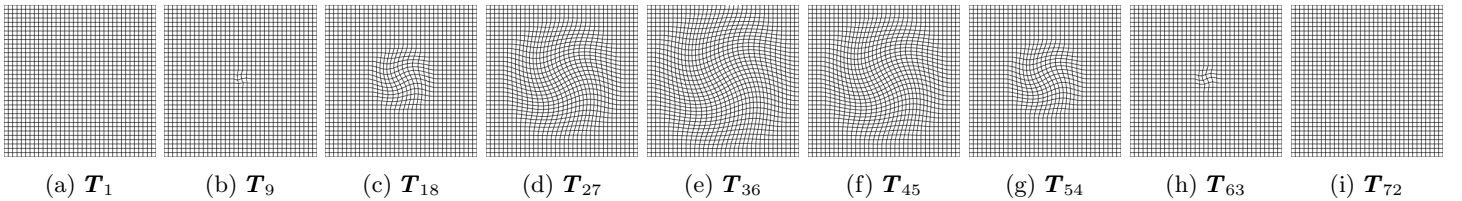
Step-1: A teapot is rotated about its vertical axis passing through the tip of its lid. Snapshots are taken from a fixed camera at 5° intervals. A total of 72 photos are taken as the teapot completes 360° rotation and return to the initial position. Each of these photos is re-sampled as a 72×72 grayscale image I_{0i} . These 72 images I_{0i} for $i = 1, \dots, 72$ are used to form a three dimensional volume image of size $72 \times 72 \times 72$. We refer to this volume image as the Rotating Teapot Image, denoted as I_0 .

Figure 15: Teapot— I_0



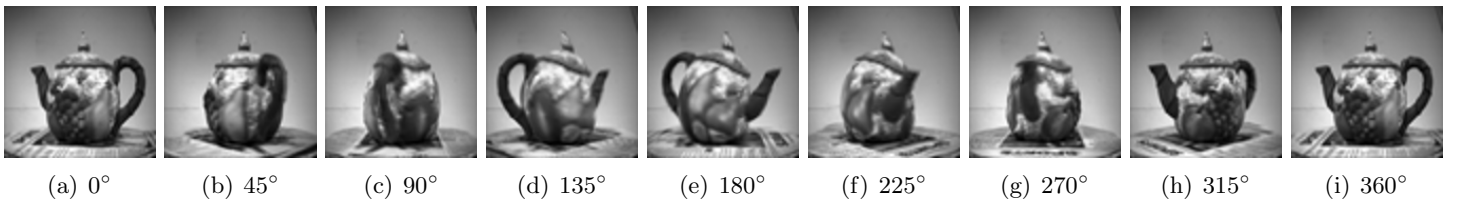
As the teapot rotates, we deform each slice I_{0i} (of I_0) to I_{ti} by a rotation \mathbf{T}_i as show in Figure 16 that is cut-off near the boundary for $i = 1, \dots, 72$.

Figure 16: \mathbf{T}_i 's



These 72 twisted 72×72 images form a $72 \times 72 \times 72$ volume image referred to as the Twisted Teapot, denoted as I_t as shown in Figure 17.

Figure 17: Twisted Teapot— $I_t = \mathbf{T}(I_0)$



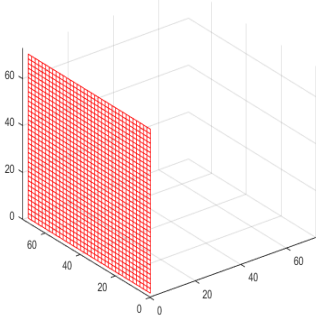
The deformations \mathbf{T}_i for $i = 1, \dots, 72$ and the Twisted Teapot image I_t can be seen from Twisted Teapot(CLICK HERE)

Step-2: The registration transformation ϕ from I_0 to I_t is calculated by minimizing

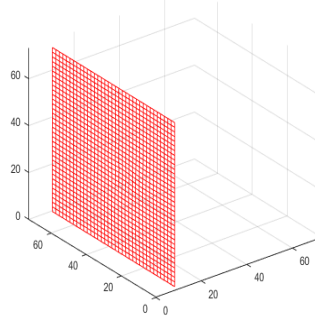
$$SSD(\phi(\mathbf{x})) = \iiint (I_t(\phi(\mathbf{x})) - I_0(\mathbf{x}))^2 d\mathbf{x} \quad (4.1)$$

The resulting registration deformation ϕ , restricted to each i th slice, is expected to be very close to \mathbf{T}_i as shown in Figure 18.

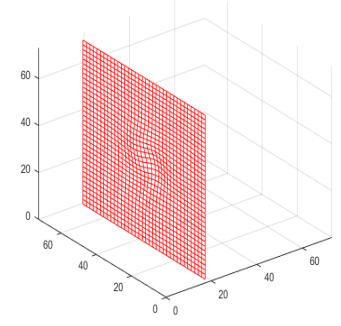
Figure 18: ϕ_i 's



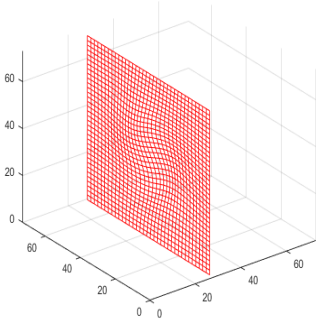
(a) ϕ_1



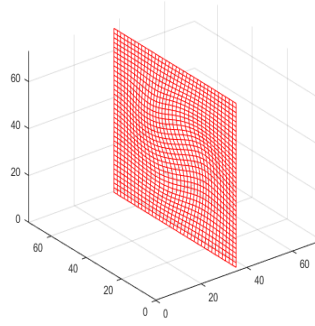
(b) ϕ_9



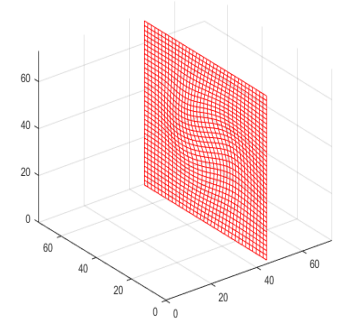
(c) ϕ_{18}



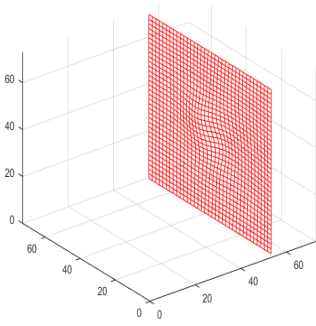
(d) ϕ_{27}



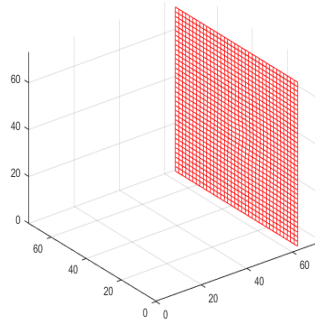
(e) ϕ_{36}



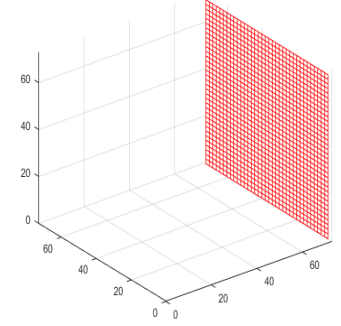
(f) ϕ_{45}



(g) ϕ_{54}



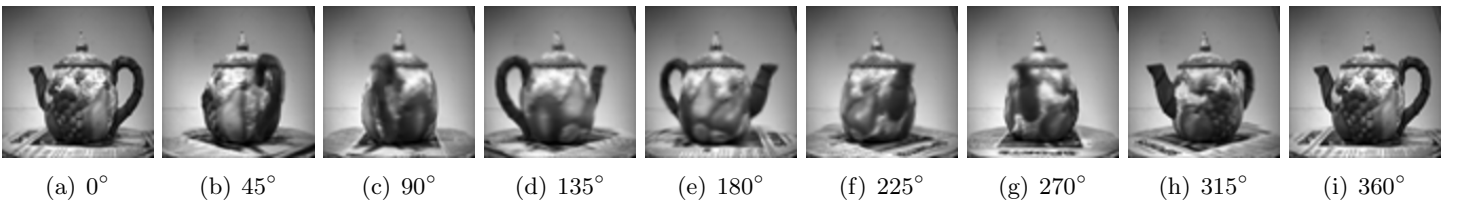
(h) ϕ_{63}



(i) ϕ_{72}

and the deformed images of the twisted teapot — $I_t(\phi)$ is expected to be close to I_0 as it shows on next Figure 19. The total elapsed time for Step-2 is 927.601032 seconds.

Figure 19: Reversed Twisted Teapot— $I_t(\phi)$



The registration deformation ϕ from Step-2 and the corresponding reversed twisted teapot image $I_t = \mathbf{T}(I_0)$ are

shown from: Reversed Twisted Teapot(CLICK HERE). From these visualization files, we conclude that our optimal control method correctly recovered the ground truth deformations \mathbf{T}_i for $i = 1, \dots, 72$ and the grand truth images I_{0i} for $i = 1, \dots, 72$, as expected.

5 Conclusion

In this paper, a set of new computational techniques is described. They are based on both the Jacobian determinant and the curl-vector. Specifically, The Variational Principle is used to calculate a transformation with prescribed Jacobian determinant and curl-vector. A new method of averaging deformations based on averaging the Jacobian determinants and the curl-vectors is used to construct an unbiased template from the members of a set of images. We will further refine the techniques and generalize them to three dimensional real world images.

References

- [1] Ashburner, J.: VBM Tutorial. <http://www.fil.ion.ucl.ac.uk/~john/misc/VBMclass10.pdf>, Mar 15, 2010.
- [2] Ashburner, J and Friston, K. J.: COMMENTS AND CONTROVERSIES, Why Voxel-Based Morphometry Should Be Used. *NeuroImage*, Vol. 14, pp. 1238-1243, 2001. doi:10.1006/nimg.2001.0961
- [3] Bookstein, F. L.: Voxel-Based Morphometry Should Not Be Used with Imperfectly Registered Images. *NeuroImage*, Vol. 14, Issue 6, pp. 1454-1462, 2001.
- [4] Hsiao, H-Y., Hsieh, C-Y., Chen, X., Gong, Y., Luo, X. and Liao, G.: New Development of Nonrigid Registration. *ANZIAM Journal*, Vol. 55, pp. 289-297, 2014. doi:10.1017/S1446181114000091
- [5] Hoshi, S., Davis, B., Jomier, M. and Gerig, G.: Unbiased Diffeomorphic Atlas Construction for Computational Anatomy *NeuroImage*, Vol. 23, pp151-160, 2004. doi:10.1016/j.neuroimage.2004.07.068
- [6] Liao, G., Cai, X., Fleitas, D., Luo, L., Wang, J. and Xue, J.: Optimal control approach to data set alignment *Applied Mathematics Letters*, Vol 21, pp. 898905, 2008
- [7] Narayana, P. A., Datta, S., Tao, G., Steinberg, J. L. and Moeller, F. G.: Effect of Cocaine on Structural Changes in Brain: MRI Volumetry using Tensor-Based Morphometry. *Drug Alcohol Depend*, Vol. 111(3), pp. 191-199, 2010.
- [8] Novak, G. and Einstein, S. G.: Structural Magnetic Resonance Imaging as a Biomarker for the Diagnosis, Progression, and Treatment of Alzheimer Disease. Janssen Research and Development, 1125 Trenton-Harbourton Road, Titusville, NJ 08560, USA. *Translational, Tools for CNS Drug Discovery, Development and Treatment*, 2013.
- [9] Sotiras, A., Davatzikos, C. and Paragios, N.: Deformable Medical Image Registration: A Survey. *IEEE TRANSACTIONS ON MEDICAL IMAGING*, VOL. 32, NO.7, Jul 2013.
- [10] Thacker, N. A.: Tutorial: A Critical Analysis of Voxel Based Morphometry (VBM). <http://www.tinavision.net/docs/memos/2003-011.pdf>, May, 2008.
- [11] Chen, X. and Liao, G.: New Variational Method of Grid Generation with Prescribed Jacobian determinant and Prescribed Curl. <http://arxiv.org/pdf/1507.03715>, 2015.
- [12] Chen, X. and Liao, G.: New method of averaging diffeomorphisms based on Jacobian determinant and curl vector. <https://arxiv.org/abs/1611.03946>, 2016.